Low Temperature Physics/Fizika Nizkikh Temperatur, 2018, v. 44, No. 7, pp. 865–876

Compact discrete breathers on flat-band networks

C. Danieli[1], A. Maluckov[1,2], and S. Flach[1,3]

[1]*Center for Theoretical Physics of Complex Systems, Institute for Basic Science, Daejeon, Korea*

[2]*Vinca Institute for Nuclear Sciences, University of Belgrade, Serbia*

[3]*New Zealand Institute for Advanced Study, Massey University, Auckland, New Zealand*
E-mail: sergejflach@googlemail.com

Received March 1, 2018, published online May 28, 2018

Linear wave equations on flat-band networks host compact localized eigenstates (CLS). Nonlinear wave equations on translationally invariant flat-band networks can host compact discrete breathers-time-periodic and spatially compact localized solutions. Such solutions can appear as one-parameter families of continued linear compact eigenstates, or as discrete sets on families of non-compact discrete breathers, or even on purely dispersive networks with fine-tuned nonlinear dispersion. In all cases, their existence relies on destructive interference. We use CLS amplitude distribution properties and orthogonality conditions to derive existence criteria and stability properties for compact discrete breathers as continued CLS.

PACS: 71.10.–w Theories and models of many-electron systems;
71.10.Fd Lattice fermion models (Hubbard model, etc.).

Keywords: compact localized eigenstates, discrete breathers, flat band.

Introduction

In recent years, flat-band tight binding networks gained interest in the fields of ultra cold atomic gases, condensed matter and photonics, among others [1]. One of the essential features of the corresponding eigenvalue problem of these linear wave equations is the presence of eigenstates which are strictly compact in space. These modes are coined *compact localized states* (CLS), and their existence is due to destructive interference which suppresses the dispersion along the network. The CLS introduce macroscopic degeneracy in the energy spectrum of the network, which results in one (or more) momentum-independent (or *dispersionless*) bands in the spectrum, hence called *flat* bands. The CLS can be found irrespective to the dimensionality of the network. CLSs can be classified according to the number U of unit cells they occupy. Class $U = 1$ CLSs form an orthogonal basis of the flat-band Hilbert space, since the compact states do not overlap. Moreover, the flat band can be freely tuned to be gapped away from dispersive bands, or to resonate with them. Class $U \geq 2$ CLSs instead typically form a non-orthogonal basis, and the flat band is gapped away (or at most touching) from dispersive bands.

Introduced by Sutherland [2] and Lieb [3] in the 1980's, and then generalized by Mielke and Tasaki in the 1990's [4,5], flat-band lattices and their perturbations provide an ideal test-bed to explore and study unconventional localization and innovative states of matter [6–8]. The effects of different types of perturbations have been studied in several examples of flat-band networks [9,10], as well as the effects of disorder and nonlinearity and interaction between them [11]. Further studies focused on non-Hermitian flat-band networks [12], topological flat Wannier–Stark bands [13], Bloch oscillations [14], Fano resonances [15], fractional charge transport [16] and the existence of nontrivial superfluid weights [17]. Chiral flat-band networks revealed that CLS and their macroscopic degeneracy can be protected under any perturbation which does not lift the bipartiteness of the network [18]. The engineering of CLS has been longly attempted [19,20], and it has been recently solved for $U = 1$ lattices [21] and for the $U = 2$ CLS in a two-band problem [22]. Experimentally, compact localized states have been realized using ultra cold atoms [23], photonic waveguides networks [24–26], exciton-polariton condensates [27,28] and superconducting wires [29,30] (for a recent survey on the state of the art, see [1].

Nonlinear translationally invariant lattices admit a class of time-periodic solutions localized in real space (typically exponentially), called *discrete breathers* [31,32]. The precise decay in the tails depends on the band structure of small amplitude linearized wave equations. For analytic band structures (usually due to short range, e.g., exponentially or faster decaying, connectivities on the lattice), the discrete breather tails decay exponentially. For non-analytic band structures (usually due to long range, e.g., algebraically decaying, connectivities on the lattice), the tails decay algebraically as well. In the absence of linear dispersion, but presence of nonlinear dispersion, tails decay superexponentially. For short range connectivities, but with acoustic parts in the band structure, and with broken space parity, the ac parts of the discrete breather tails decay exponentially, while the dc part (static lattice deformation) will decay algebraically [31,32].

A natural question then arises whether discrete breathers can have strictly zero tails, and turn into compact excitations. For instance, traveling solitary waves with compact support have been found in the frame of spatially continuous partial differential equations by Rosenau and Hyman in the Korteweg–de Vries model [33]. In discrete systems, spatially compact time-periodic solutions have been found by Page in a purely anharmonic one-dimensional *Fermi–Pasta–Ulam*-like chain in the limit of non-analytic compact (box) interaction potential [34]. Moreover, Kevrekidis and Konotop reported on compact solutions in translationally invariant one-dimensional lattices in the presence of non-local nonlinear terms [35]. In this work, we consider flat-band networks as the underlying support for compact time-periodic excitations.

The existence of compact discrete breathers in nonlinear flat-band networks was observed in [36,37]. Furthermore, the coexistence between nonlinear terms and spin-orbit coupling has been discussed in the framework of ultra-cold atoms in a diamond chain [38]. Perchikov and Gendelman studied compact time-periodic solutions in a one-dimensional nonlinear mechanical cross-stitch network [39]. In this case the above mentioned destructive interference translates into several time-dependent forces acting on masses in the mechanical network in such a way that the sum of all forces vanishes, leading to a compactification of the vibrational excitation.

In this work, we present a necessary and sufficient condition for the existence and continuation of time-periodic and compact in space solutions (herewith called *compact discrete breather*) on flat-band networks with local nonlinearity. The existence and continuation condition applies irrespective of the dimensionality of the lattice and the class U of linear CLS. Then, we discuss the linear stability of compact discrete breathers. For orthogonal CLSs in $U = 1$ networks, the only source of instability are resonances with extended states. For class $U \geq 2$ networks instead, the non-orthogonality between linear CLSs induces additional potential local instabilities due to CLS-CLS interaction. Resonances with dispersive states lead to radiation and potential complete annihilation. Resonances with neighboring CLSs in general simply yield local instabilities which do not annihilate the excitation. The study of the nonlinear stability has been performed numerically, and standard techniques of perturbation theory have been applied to substantiate the numerical findings. The present work is structured as follows: in Sec. 1 we will present the flat-band networks; then in Sec. 2 we introduce the nonlinear terms in flat-band model equations, and discuss the continuation criteria of linear CLS to compact discrete breathers. Next, in Sec. 3 we present the linear stability analysis of the compact discrete breathers, which will then be discussed numerically in Sec. 4.

1. Flat-band networks

For simplicity we will operate in one spatial dimension. Results in general take over to higher dimensions. We will comment on particular cases where caution is to be executed. The linear time-dependent model equation of the flat-band networks can be presented in a form

$$i\dot{\psi}_n = H_0\psi_n + H_1\psi_{n+1} + H_1^\dagger\psi_{n+1}. \tag{1}$$

For all $n \in \mathbb{Z}$, $\psi_n \in \mathbb{C}^\nu$ is a time-dependent complex vector of ν components, each one representing one site of the network. The set of ν sites is called the *unit-cell*. The matrix H_0 defines the geometry of the unit-cell, while the matrixes H_1, $H_1^\dagger$ define the hopping between nearest-neighboring ones. This model equation can be easily generalized to longer range hopping, as well as higher dimensional networks. The phase-amplitude ansatz $\psi_n(t) = A_n e^{-iEt}$ leads to the associated eigenvalue problem

$$EA_n = H_0A_n + H_1A_{n+1} + H_1^\dagger A_{n+1}. \tag{2}$$

Then, the Bloch solution $A_n = \varphi_q e^{iqn}$ of Eq. (2) defined for the wave-vector q gives rise to the Bloch Hamiltonian of the lattices

$$E\varphi_q = H(q)\varphi_q \equiv [H_0 + e^{iq}H_1 + e^{-iq}H_1^\dagger]\varphi_q. \tag{3}$$

Equation (3) yields the band structure $E = \cup_{i=1}^{\nu} E_i(q)$ of the problem. We consider lattices which exhibit at least one band independent from the wave vector q, which we call disperionless (or *flat*) band E_{FB}. The eigenmodes associated to a flat-band are typically compact localized states, and the number U of unit-cells occupied by one CLS is the flat band *class*. These states can be written in the time-dependent form solutions of Eq. (1):

$$\psi_{n,n_0}(t) = \left[\sum_{l=0}^{U-1} v_l \delta_{n,n_0+l}\right] e^{-iE_{FB}t}, \tag{4}$$

where the sum indicates the spatial component of the CLSs. The real vectors v_l are defined as the following:

$$v_l = \sum_{j=1}^{\nu} a_{l,j} A_{l,j} \mathbf{e}_j, \tag{5}$$

where the vectors $\{\mathbf{e}_j\}_{j=1}^{\nu}$ form the canonical basis of $\mathbb{R}^{\nu} = \langle \mathbf{e}_1, \ldots, \mathbf{e}_{\nu} \rangle$; $a_{l,j} \in \{0, \pm 1\}$ denotes the sites with non-zero amplitude, and the real numbers $A_{l,j} \in \mathbb{R}$ defines the amplitudes in the sites with non-zero $a_{i,j}$. In the next section, we will introduce local nonlinear terms to Eq. (1), and we will discuss continuation criteria for the CLS introduced in Eq. (4) as compact solution of the nonlinear regime.

2. Nonlinear flat-band networks and continuation of compact localized states

Let us consider the model equation of the flat-band network Eq. (1) in presence of local nonlinear terms

$$i\dot{\psi}_n = H_0 \psi_n + H_1 \psi_{n+1} + H_1^{\dagger} \psi_{n+1} + \gamma \mathcal{F}(\psi_n) \psi_n, \tag{6}$$

where the matrix $\mathcal{F}(\psi_n)$

$$\mathcal{F}(\psi_n) \equiv \sum_{j=1}^{\nu} |\psi_n^j|^2 \, \mathbf{e}_j \otimes \mathbf{e}_j \tag{7}$$

contains the terms $|\psi_n^i|^2$ along the diagonal. We seek for time-periodic solutions of the nonlinear system Eq. (6)

$$C_{n,n_0}(t) = \left[\sum_{l=0}^{U-1} v_l \delta_{n,n_0+l} \right] e^{-i\Omega t} \tag{8}$$

with frequency Ω, which are continuation of the CLSs Eqs. (4), (5) that exist in the linear regime $\gamma = 0$.

We consider the compact solution (8) defined with the profile in space of the linear CLS in Eqs. (4), (5) and frequency Ω, and check under which conditions these are solutions of the nonlinear equation (6). At first, let us observe that for all sites where a CLS is zero ($a_{l,j} = 0$ and outside the range of U cells in Eq. (4)), Eq. (6) is solved. For $l = 1, \ldots, U$ and $j = 1, \ldots, \nu$ where a CLS has non-zero amplitude $a_{l,j} \neq 0$, Eq. (6) reduces to

$$\Omega A_{l,j} = E_{FB} A_{l,j} + \gamma A_{l,j}^3. \tag{9}$$

If for all l, j such that $a_{l,j} \neq 0$, $|A_{l,j}| \equiv A$ (all sites have same amplitude in absolute value), Eq. (9) turns into

$$A^2 = \frac{\Omega - E_{FB}}{\gamma}. \tag{10}$$

If instead there exist non-zero $|A_{l,j}| \neq |A_{\hat{l},\hat{j}}|$, Eq. (9) yields different frequencies Ω, which breaks the condition of continuation of CLS as a periodic orbit with compact support. Let us introduce the following definition:

Definition: let $\psi_{n,n_0}(t)$ be a CLS of class U of a flat-band network with ν sites per unit-cell. We call $\psi_{n,n_0}(t)$ a *homogeneous* CLS if

$$\text{for all } a_{l,j} \neq 0 \;\Rightarrow\; |A_{l,j}| \equiv A \tag{11}$$

and we call $\psi_{n,n_0}(t)$ a *heterogeneous* CLS otherwise.

From the above consideration in Eqs. (9), (10), we can obtain the following continuation criteria in the following lemma:

Lemma: in a nonlinear flat-band network Eq. (6), a compact state $\psi_{n,n_0}(t)$ of the linear lattice $\gamma = 0$ with energy E_{FB} can be continued as a periodic orbit with compact support $C_{n,n_0}(t)$ with frequency $\Omega = E_{FB} + \gamma A^2$ *if and only if* it is homogeneous.

This lemma states a necessary and sufficient condition for linear CLSs to be continued as time-periodic solutions of the nonlinear regime with compact support. Indeed, *homogeneous* CLSs in presence of this local nonlinearity do not break the destructive interference, preserving therefore the compactness in space. *Heterogeneous* CLSs instead in presence of nonlinearity break the destructive interference, loosing therefore the compactness in space. We call the continued homogeneous CLS solutions *compact discrete breathers*. Their spatial profile is identical to the CLS one, and their frequency is given by

$$\Omega = E_{FB} + g, \qquad g \equiv \gamma A^2. \tag{12}$$

In the next section, we will discuss the linear stability of compact discrete breathers.

3. Linear stability analysis

Herewith, we consider a perturbation $\varepsilon_n(t)$ of a compact discrete breather $C_{n,n_0}(t)$ Eq. (8) solution of the nonlinear flat-band model (6)

$$\psi_n(t) = C_{n,n_0}(t) + \varepsilon_n(t). \tag{13}$$

By linearizing Eq. (6) around one compact discrete breather $C_{n,n_0}(t)$, and defining $g \equiv \gamma A^2$, we obtain

$$i\dot{\varepsilon}_n = H_0 \varepsilon_n + H_1 \varepsilon_{n+1} + H_1^{\dagger} \varepsilon_{n+1} + g \sum_{l=0}^{U-1} \Gamma_l \left(2\varepsilon_n + e^{-i2\Omega t} \varepsilon_n^* \right) \delta_{n,n_0+l}, \tag{14}$$

where $\{\Gamma_l\}_{l=0}^{U-1}$ are the projector operators of ψ_n over a compact discrete breather $C_{n,n_0}(t)$

$$\Gamma_l = \sum_{j=1}^{\nu} a_{l,j} \mathbf{e}_j \otimes \mathbf{e}_j. \tag{15}$$

The resulting dynamical model Eq. (14) for the perturbation term ε_n consists of equations with time-dependent coefficients that occur at sites where the compact discrete breather $C_{n,n_0}(t)$ has non-zero amplitudes. The aim of this section is to analytically prove the existence of regions of instability in the parameter space $(\Omega, g) \in \mathbb{R} \times \mathbb{R}$ for the compact discrete breather. In order to achieve this, we first express Eq. (14) in the Bloch representation. Than, we compute the condition for resonance determining the Floquet

matrix at $g = 0$. At last, we obtain the regions of instability around the resonances via the strained coefficient method, focusing on the $U = 1$ and $U = 2$ cases.

3.1. Bloch states representation

Let us consider the Bloch representation of Eq. (14) using the following transformation:

$$\varepsilon_n = \frac{1}{\sqrt{N}} \sum_q \phi_q e^{iqn}. \tag{16}$$

This leads to the Bloch equation,

$$i\dot{\phi}_{\hat{q}} = H(\hat{q})\phi_{\hat{q}} + \\ + \frac{g}{N} \sum_q \left[\sum_{l=0}^{U-1} e^{-i\hat{q}l} \Gamma_l \left(2e^{iql} \phi_q + e^{-i2\Omega t} e^{-iql} \phi_q^* \right) \right], \tag{17}$$

where $H(q) \equiv H_0 + e^{iq} H_1 + e^{-iq} H_1^\dagger$ is the Bloch matrix. The $H(q)$ matrix admits ν eigenvectors v_q^i and ν eigenvalues λ_q^i. We assume that one flat band $\lambda_q^1 = E_{FB}$ exists with corresponding eigenvector w_q of the Bloch matrix. Then we define the expansion of $\phi_{\hat{q}}$ in the Bloch eigenbasis

$$\phi_{\hat{q}} = f_{\hat{q}} w_{\hat{q}} + \sum_{i=2}^{\nu} d_{\hat{q}}^i v_{\hat{q}}^i. \tag{18}$$

The resulting equations on the expansion coefficients $f_{\hat{q}}$ of the flat band reads (see Appendix A)

$$i\dot{f}_{\hat{q}} = E_{FB} f_{\hat{q}} + \\ + \frac{g}{N} \sum_q \left\{ \sum_{l=0}^{U-1} e^{-i\hat{q}l} \left(2e^{iql} f_q + e^{-i2\Omega t} e^{-iql} f_q^* \right) \Gamma_l w_q w_q^* + \right. \\ \left. + \sum_{l=0}^{U-1} \left[\sum_{i=2}^{\nu} e^{-i\hat{q}l} \left(2e^{iql} d_q^i + e^{-i2\Omega t} e^{-iql} d_q^{i*} \right) \Gamma_l v_q^i w_q^* \right] \right\} \tag{19}$$

while the equation of the coefficients $d_{\hat{q}}$ of the jth dispersive band reads

$$\dot{d}_{\hat{q}}^j = \lambda_{\hat{q}}^j d_{\hat{q}}^j + \\ + \frac{g}{N} \sum_q \left\{ \sum_{l=0}^{U-1} e^{-i\hat{q}l} \left(2e^{iql} f_q + e^{-i2\Omega t} e^{-iql} f_q^* \right) \Gamma_l w_q \cdot v_q^{j*} + \right. \\ \left. + \sum_{l=0}^{U-1} \left[\sum_{i=2}^{\nu} e^{-i\hat{q}l} \left(2e^{iql} d_q^i + e^{-i2\Omega t} e^{-iql} d_q^{i*} \right) \Gamma_l v_q^i \cdot v_q^{j*} \right] \right\}. \tag{20}$$

Equations (19) and (20) describe the time-dynamics of the flat-band states f_q with dispersive states d_q^i due to the linearized term of Eq. (14). For class $U = 1$, these equations are decoupled, while for class $U > 1$ they are coupled. In the next subsection, we neglect the terms following from the nonlinearity (set $g = 0$), and obtain the resonance condition by computing the Floquet matrix of the system Eqs. (19), (20).

3.2. Floquet matrix

For $g = 0$, we calculate the *Floquet matrix A* for Eqs. (19), (20) (also called *period advancing matrix*). For $\varphi = (f_q, d_q)$ and $T = \pi / \Omega$, it follows that

$$\begin{bmatrix} \varphi(t+T) \\ \varphi^*(t+T) \end{bmatrix} = A \begin{bmatrix} \varphi(t) \\ \varphi^*(t) \end{bmatrix} \quad \text{with} \quad A \equiv \begin{bmatrix} e^{-i\lambda T} & 0 \\ 0 & e^{i\lambda T} \end{bmatrix}. \tag{21}$$

The eigenvalues of the Floquet matrix A will be degenerate on the unit circle *if and only if* $\cos^2(\lambda T) = 1$, which means

$$\cos^2(\lambda T) = 1 \quad \Leftrightarrow \quad \lambda T = m\pi, \quad m \in \mathbb{Z}, \\ \Leftrightarrow \quad \lambda = m\Omega, \quad m \in \mathbb{Z}. \tag{22}$$

Concerning Eqs. (19), (20), Eq. (22) implies that for $m \in \mathbb{Z}$

$$E_{FB} = m\Omega, \qquad \lambda_q^j = m\Omega, \qquad j = 2, \ldots, \nu. \tag{23}$$

It follows that from the values of the frequency Ω of a compact discrete breather $C_{n,n_0}(t)$ contained in Eq. (23), regions of instability (Arnol'd tongues) in the parameter space (Ω, g) are expected. In order to obtain an approximation of these regions, we apply a standard technique of perturbation theory called strained method coefficient.

3.3. Arnol'd tongues

In the following, we estimate the regions of instability in the parameter space (Ω, g) of Eqs. (19) and (20), separating between the class $U = 1$ case (where the dispersive states are decoupled from the flat-band ones) and the class $U = 2$ case (where dispersive and flat-band states are coupled).

3.3.1. Class U = 1

In the case of class $U = 1$ flat-band network, it holds that $\Gamma_0 w_q = w_q$ and Eqs. (19), (20) reduce to

$$i\dot{f}_{\hat{q}} = E_{FB} f_{\hat{q}} + \frac{g}{N} \sum_q \left(2e^{iql} f_q + e^{-i2\Omega t} e^{-iql} f_q^* \right), \\ i\dot{d}_{\hat{q}}^j = \lambda_{\hat{q}}^j d_{\hat{q}}^j + \frac{g}{N} \sum_{i=2}^{\nu} \left\{ \sum_q 2d_q^i + e^{-i2\Omega t} d_q^{i*} \right\} \Gamma_0 v_q^i \cdot v_q^{j*}. \tag{24}$$

Without loss of generality, we refer to a two bands problem $\nu = 2$. The equations of the dispersive band component d_q of Eq. (24) read

$$i\dot{d}_{\hat{q}} = \lambda_{\hat{q}} d_{\hat{q}} + \frac{g}{N}\sum_q \left(2d_q + \mathrm{e}^{-i2\Omega t} d_q^*\right). \qquad (25)$$

The strained coefficient method consists in expanding in powers of g both the time-dependent component d_q as well as the frequency term $\lambda_{\hat{q}}$ around one of the resonant frequencies in Eq. (23). Then, we determine the expansion coefficients so that the resulting expansion is periodic. This will define transition curves between stability and instability regions in the parameter space (Ω, g) (for further details, see [40]). The expansion of $d_{\hat{q}}$ and $\lambda_{\hat{q}}$ reads

$$d_{\hat{q}} = \sum_{k=0}^{+\infty} g^k u_k^{(\hat{q})}, \qquad \lambda_{\hat{q}} = m\Omega + \sum_{l=1}^{+\infty} g^l \delta_l \qquad (26)$$

for $\lambda_{\hat{q}} \neq \lambda_q$ and for all $q \neq \hat{q}$. Vanishing the *secular terms* (terms which give rise to non-periodicities in the expansion) demands the following conditions in the expansion coefficient δ_1 (see Appendix B for details)

$$\delta_1 = -\frac{3}{N}, -\frac{1}{N}, \qquad m = 1,$$
$$\delta_1 = -\frac{2}{N}, \qquad m \neq 1. \qquad (27)$$

This implies that a region of instability appears from each dispersive frequency λ_q (obtained for $m = 1$ in Eq. (23)), while for λ_q / m for $m \geq 2$ regions of instability are absent. It is important to notice that for $N \mapsto \infty$ the coefficients in Eq. (27) converge to zero, implying that in the limit of infinite chain, the instability regions disappear, in analogy with [41]. In Fig. 1 we can see a representation of the Arnol'd tongue around one frequency λ_q.

Analogous conclusions follow from the strained coefficient method applied to the flat-band states f_q. Here the expansions reads

$$f_{\hat{q}} = \sum_{k=0}^{+\infty} g^k v_k^{(\hat{q})}, \qquad E_{FB} = m\Omega + \sum_{l=1}^{+\infty} g^l \sigma_l. \qquad (28)$$

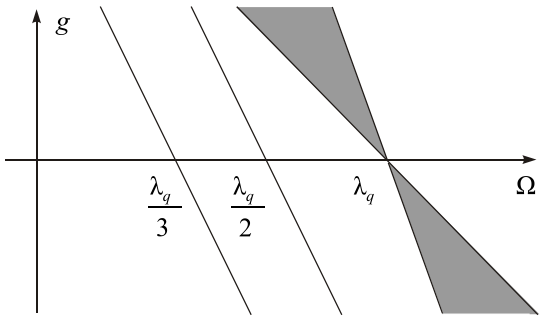

Fig. 1. First order approximation of the Arnold's tongues (grey shaded area) at a dispersive energy λ_q.

The zeroing of the secular terms yields to the following coefficients:

$$\sigma_1 = -3, -1, \qquad m = 1,$$
$$\sigma_1 = -2, \qquad m \neq 1. \qquad (29)$$

Equation (29) is independent on N due to macroscopic degeneracy of the flat-band states (see Appendix B for details).

The strained coefficient method showed the appearance of regions of instability in correspondence of each dispersive energy λ_q of the dispersive band. However, instability regions do not appear for higher order resonances (λ_q / m for $m \geq 2$) (see Fig. 1). Furthermore, we can notice that this region of instability also follows from the Bogoliubov expansion of Eq. (24) (see Appendix C for details). Before to go ahead to numerical studies, we briefly check the previous approach in the case with $U = 2$.

3.3.2. Class $U \geq 2$

In the case $U = 2$, without loss of generality, we refer to a two band problem $\nu = 2$, using the saw-tooth network as a test-bed. Equations (19), (20) read (see Appendix B for details)

$$i\dot{f}_{\hat{q}} = E_{FB} f_{\hat{q}} + \frac{g}{\alpha^2 N}\sum_q \left\{\left(\alpha^2 - 1\right)\left(f_q + \mathrm{e}^{-i2\Omega t} f_q^*\right) + \right.$$
$$+ \mathrm{e}^{-i\hat{q}}\left(2\mathrm{e}^{iq} f_q + \mathrm{e}^{-i2\Omega t}\mathrm{e}^{-iq} f_q^*\right) +$$
$$\left. + \left(1 + \mathrm{e}^{-iq}\right)\left(2d_q^i + \mathrm{e}^{-i2\Omega t} d_q^{i*}\right)\right\}, \qquad (30)$$

$$i\dot{d}_{\hat{q}} = \lambda_q d_{\hat{q}} + \frac{g}{\alpha^2 N}\sum_q \left\{\left(2d_q + \mathrm{e}^{-i2\Omega t} d_q^*\right) + \right.$$
$$+ \mathrm{e}^{-i\hat{q}}\left(2\mathrm{e}^{iq} d_q + \mathrm{e}^{-i2\Omega t}\mathrm{e}^{-iq} d_q^*\right) +$$
$$\left. + \left(1 + \mathrm{e}^{iq}\right)\left(2 f_q + \mathrm{e}^{-i2\Omega t} f_q^*\right)\right\} \qquad (31)$$

for $\alpha = \sqrt{3 + 2\cos q}$. Both expansions Eqs. (26), (28) have to be applied to Eqs. (30), (31). However, in the first order, the additional terms (the second and the third lines of both equations) do not provide the appearance of further regions of instability (see Appendix B for details). These additional *polarized* terms (terms dependent on the wave number q) indeed provide interactions between dispersive and flat-band states. However, the strained coefficient method does not report additional instability regions in the parameter space (Ω, g) due to these terms. In the following, we will discuss numerically the linear stability of the compact discrete breather solutions of certain examples of class $U = 1$ and class $U = 2$ one-dimensional nonlinear flat-band networks.

4. Numerical results

In this section we numerically study the linear stability properties of the compact discrete breather solutions of certain flat-band topologies. We then relate the numerical observations with the analytical results discussed above. Herewith we numerically solve the eigenvalue problem Eq. (14) obtained from the time-evolution Eq. (6) linearized around a compact discrete breather Eq. (13). Generally, we will obtain complex eigenvalues, and the presence of non-zero real part will highlight instability [42]. We will also discuss the nature of the eigenvector associated to unstable eigenvalues (eigenvalues with non-zero real part). Furthermore, we will substantiate the findings by showing simulations of the time evolution of initially perturbed compact discrete breathers. In the following, we will focus on two models: the *cross-stitch* lattice and the *saw-tooth* chain. In Appendix D we detail the numerical methods used along the work.

4.1. Cross-stitch lattice

The cross-stitch lattice (Fig. 2(a)) is a one-dimensional two-band network, which possesses one flat band. Associated to the flat band, there exists a countable set of class $U=1$ compact localized states, whose homogeneous profile in space is shown by the black dots in Fig. 2(a). The full band structure of the model is

$$E_{FB}=h, \qquad E(q)=-h+4\cos(q) \tag{32}$$

which can be visualized in Fig. 2(b), for $h=3$. In this model, the relative position between dispersive and flat bands can be tuned using the free parameter $h\in\mathbb{R}$, which leads to crossing between the two bands for $|h|<2$, band touching for $|h|=2$, and presence of a band gap for $|h|>2$.

The time-dependent equations of the cross-stitch lattice in the presence of onsite nonlinearity read

$$\begin{aligned} i\dot{a}_n &= -a_{n-1}-a_{n+1}-b_{n-1}-b_{n+1}-hb_n+\gamma a_n|a_n|^2,\\ i\dot{b}_n &= -a_{n-1}-a_{n+1}-b_{n-1}-b_{n+1}-ha_n+\gamma b_n|b_n|^2, \end{aligned} \tag{33}$$

where γ is the nonlinearity strength. As we have in Sec. 2, the CLSs of the linear regime can be continued as compact discrete breathers written as Eqs. (4), (5) with frequency $\Omega=E_{FB}+\gamma A^2$:

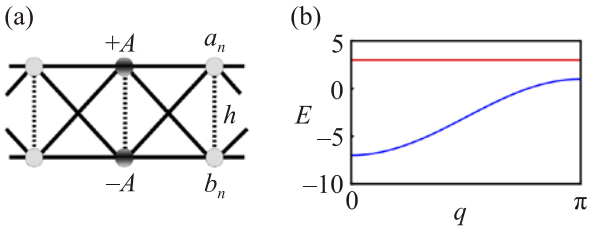

Fig. 2. (a) Profile of the cross-stitch lattice. (b) Band structure for $h=3$.

$$\mathcal{C}_{n,n_0}(t)=A\begin{pmatrix}1\\-1\end{pmatrix}\delta_{n,n_0}e^{-i\Omega t}. \tag{34}$$

In order to study the linear stability of this model, we linearize Eq. (33) around the compact discrete breathers Eq. (34), and we numerically calculate the eigenenergies of the resulting model for different values of $g=\gamma A^2$ (obtained fixing $A=1$).

The outcome of our computations can be phrased in the following way. Consider first a weakly nonlinear compact discrete breather with $|g|\ll 1$. Due to $U=1$ the linear CLS states are all degenerate but span an orthonormal eigenvector basis of the flat-band Hilbert subspace. Therefore, the degeneracy is harmless, and continuing one CLS into the nonlinear regime will not lead to any resonant interactions with neighboring CLSs. Therefore, a compact discrete breather whose frequency Ω is not in resonance with the dispersive part of the linear spectrum $E(q)$ is linearly stable. However, if a compact discrete breather is tuned into resonance with the dispersive part of the linear spectrum, it will become linearly unstable due to the resonance with extended dispersive states. If we tune the nonlinearity to a finite strength, non-perturbative effects will lead to additional instability windows for compact discrete breathers.

In Fig. 3, we show the time evolution of perturbed compact discrete breathers. We choose the amplitude of the compact breather to initially be $A=1$, and then we introduce an initial uniform random perturbation with maximum amplitude 10^{-3} along the whole chain of $N=50$ unit-cells. In Figs. 3(a) and (b) we show the time evolution of the $|a_n(t)|$ component for $h=3$, $g=5$ and $h=1$, $g=1$, respectively. Plot (a) has been obtained for $h=3$ and $g=5$, when the frequency $\Omega=3+5=8$ of the compact discrete breather is located outside the dispersive band [–7,1]. The numerical

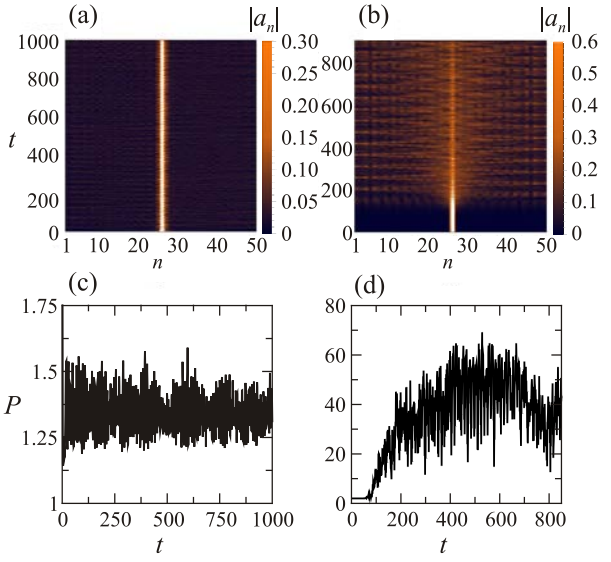

Fig. 3. (Color online) Cross-stitch: (a) and (b): Time evolution of the components $a_n(t)$ of an initially perturbed compact breathers. (c) and (d): Time evolution of the participation number P. Plots correspond to: $h=3$, $g=5$ (a), (c); $h=1$, $g=1$ (b), (d).

simulation of the time-evolution shows stability of the compact breather. Instead, plot (b) has been obtained for $h = 1$, and $g = 1$, when the frequency $\Omega = 1+1 = 2$ of the compact breather is in resonance with the dispersive band [–5,3]. The breather will start to radiate and reduce its amplitude, however the resonance condition will not be destroyed down to the linear level since the linear flat band is resonating with the dispersive one. Thus the compact discrete breather is unstable and will be completely destroyed during its perturbed evolution. The stable and the unstable behavior of these two cases are confirmed in Figs. 3(c) and (d), where we show the time evolution of the participation number $P = 1/\sum\left(|a_n|^4 + |b_n|^4\right)$. The participation number takes values between unity (obtained for a single site excitation) to the system size (obtained for uniformly excited states), $P \in [1, N]$, and it estimates the number of non-negligibly excited sites. Indeed, in plot (c) which corresponds to the stable compact discrete breather shown in Fig. 3(a), the participation number P fluctuates around 1.5, confirming that only few sites are excited. In plot (d), which corresponds to the unstable compact discrete breather shown in Fig. 3(b), the participation number P fluctuates around 40, confirming the loss of compactness and the instability of the compact breather.

4.2. Saw-tooth

The saw-tooth lattice [Fig. 4(a)] is a one-dimensional two-band network with one flat band. Associated to the flat band, there exists a countable set of class $U = 2$ compact localized states, whose homogeneous profile in space is shown by the black dots in Fig. 4(a). We recall that in this network, every CLS is non-orthogonal with its two nearest neighbors. The full band structure of the model is

$$E_{FB} = 1, \qquad E(q) = -2 - 2\cos(q) \tag{35}$$

which can be observed in Fig. 4(b). Differently from the cross-stitch case, the spectral bands of this model cannot be tuned by certain free parameter, and the network possesses a band gap between the dispersive and the flat band.

The time-dependent equations (6) of the saw-tooth in presence of onsite nonlinearity read

$$i\dot{a}_n = -b_n - b_{n+1} + \gamma a_n |a_n|^2,$$
$$i\dot{b}_n = -b_n - b_{n-1} - b_{n+1} - a_{n-1} - a_n + \gamma b_n |b_n|^2 . \tag{36}$$

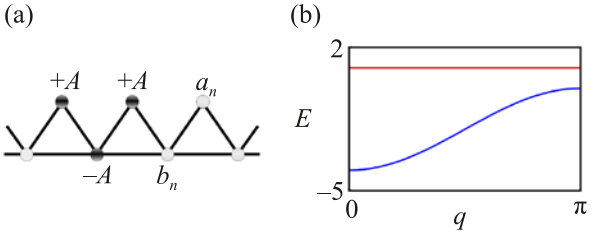

Fig. 4. (a) Profile of the saw-tooth lattice. (b) Band structure.

The CLSs of the linear regime can be continued as compact discrete breathers written Eqs. (4), (5) with frequency $\Omega = E_{FB} + \gamma A^2$ written as

$$\mathcal{C}_{n,n_0}(t) = A\left[\begin{pmatrix}1\\0\end{pmatrix}\delta_{n,n_0-1} + \begin{pmatrix}1\\-1\end{pmatrix}\delta_{n,n_0}\right]e^{-i\Omega t}. \tag{37}$$

Comparing to the $U = 1$ case of the cross-stitch lattice, the new feature is the non-orthogonality of neighboring CLSs at the linear limit. While the flat band is gapped away from the dispersive band, at weak nonlinearities we can expect a resonant interaction between neighboring CLSs, which may, or may not, lead to model dependent linear local instability. It turns out that this instability indeed takes place for the saw-tooth chain. There exists a narrow region of instability for $-0.1 < g < 0$. Therefore, the fact that the linear flat-band network is of class $U = 2$ makes compact discrete breathers unstable even in the presence of a band gap. However, this instability is local, and therefore might not lead to a destruction of the perturbed compact discrete breather, since there is no way to radiate the excitation to infinity. In Fig. 5 we show the a_n components (a) and the b_n components (b) of the unstable eigenvector with pure real eigenvalue $EV = 2.987\cdot10^{-5}$ obtained for $g = -0.001$. The eigenvector is exponentially localized.

Let us discuss the time evolution of slightly perturbed compact discrete breathers, where a perturbation of order 10^{-3} is equidistributed along all the $N = 50$ unit-cells. In Figs. 6(a) and (b), we show the time evolution of the $|a_n(t)|$ component for $g = -1.5$ and $g = -0.007$, respectively, while in Figs. 6(c) and (d) we show the time evolution of the participation number P. In the left column, Figs. 6(a) and (c) correspond to the time evolution of a compact discrete breather for $g = -1.5$. In this case, the compact discrete breather is unstable, since its frequency $\Omega = 1-1.5 = -0.5$ is in resonance with the dispersive band $[-4, 0]$. This instability is also depicted by the participation number P. In the right column, Figs. 6(b) and (d), we plot the time evolution of a compact discrete breather for $g = -0.007$. In this case, the pure real eigenvalues and the exponentially localized eigenvector yield an oscillatory behavior in time of the compact discrete breather, which is depicted also by the participation number P.

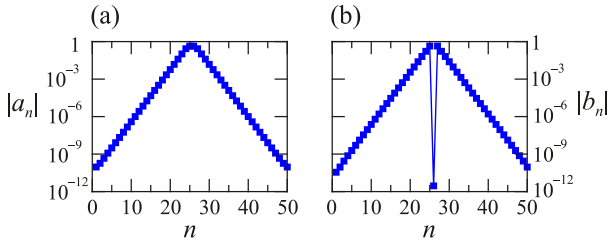

Fig. 5. Saw-tooth: a_n component (a) and b_n component (b) of the unstable eigenvector for $g = -10^{-3}$ and real eigenvalue $EV = 2.987\cdot10^{-5}$.

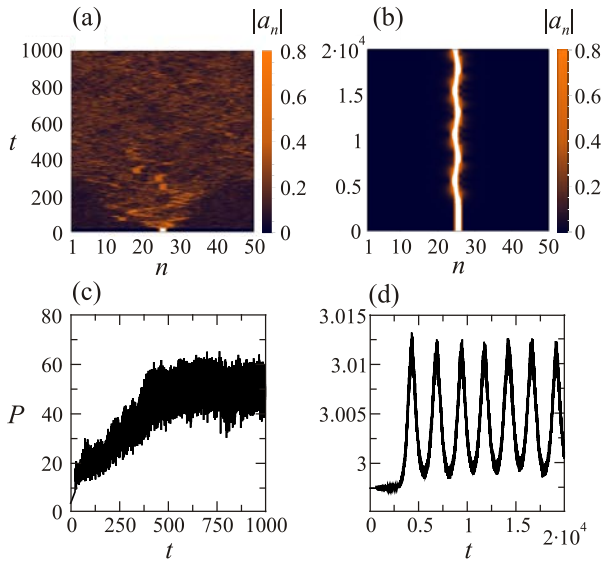

Fig. 6. (Color online) Saw-tooth. Time evolution of the amplitudes of perturbed compact breathers (component $|a_n(t)|$) and the participation number. Plots correspond to: $g = -1.5$ (a), (c) $g = -7\cdot10^{-3}$ (b), (d).

5. Conclusions

In this work, we have discussed the properties of compact discrete breathers in some flat-band networks. Linear flat-band networks possess compact localized states. In order to continue them into the nonlinear regime to become compact discrete breathers, a homogeneity condition on the amplitude distribution of CLS has to be satisfied, which is known to be present for a number of flat-band networks. The nonlinear compact discrete breathers will then persist as compact states, albeit with tuned modified frequencies.

If these frequencies are in resonance with dispersive branches of the linear flat-band network, then the discrete breather will turn linearly unstable, which may lead to a complete destruction of the perturbed breather by dissolving it into dispersive states. If the CLSs form an orthonormal set at the linear limit, no further instabilities are expected in the weakly nonlinear regime. So all it is needed to have a stable compact discrete breather at the weakly nonlinear limit, is to tune the flat-band energy out of resonance with the dispersive bands.

However, there exist flat-band networks for which the CLSs are not orthogonal. In these cases, the flat band is gapped away from the dispersive spectrum, and resonances with the dispersive spectrum are avoided in the weakly nonlinear regime. But the overlap with nearest neighbor CLS states can lead to a local instability in the weakly nonlinear regime. We indeed observe that this is the case for the saw-tooth chain. Remarkably the instability does not lead to a complete destruction of the breather, and instead yields a local oscillation of the excitation.

The class of heterogeneous CLSs cannot be continued as compact discrete breathers. However, as discussed in [36], flat-band networks that admit heterogeneous CLSs in presence of local nonlinearity admit families of exponentially localized discrete breathers. Additional fine-tuning of parameters and functions can lead to a compactification for a countable set of discrete breathers.

Acknowledgments

The authors acknowledge financial support from IBS (Project Code No. IBS-R024-D1). A.M. acknowledges support from the Ministry of Education and Science of Serbia (Project III45010).

Appendix A: Bloch states representation

Let us consider Eq. (6) linearized around one compact discrete breather $C_{n,n_0}(t)$, for $g \equiv \gamma A^2$

$$i\dot{\varepsilon}_n = H_0\varepsilon_n + H_1\varepsilon_{n+1} + H_1^{\dagger}\varepsilon_{n+1} + \\ + g\sum_{l=0}^{U-1}\Gamma_l(2\varepsilon_n + \mathrm{e}^{-i2\Omega t}\varepsilon_n^*)\delta_{n,n_0+l}, \tag{A1}$$

where $\{\Gamma_l\}_{l=0}^{U-1}$ are the projector operators of the vector ψ_n over a compact discrete breather $C_{n,n_0}(t)$:

$$\Gamma_l = \sum_{j=1}^{\nu} a_{l,j}\mathbf{e}_j \otimes \mathbf{e}_j. \tag{A2}$$

The expansion Eq. (16) in Bloch states

$$\varepsilon_n = \frac{1}{\sqrt{N}}\sum_q \phi_q \mathrm{e}^{iqn} \tag{A3}$$

maps Eq. (A1) to

$$i\frac{1}{\sqrt{N}}\frac{\partial}{\partial t}\sum_q \phi_q \mathrm{e}^{iqn} = \frac{1}{\sqrt{N}}\sum_q H(q)\phi_q \mathrm{e}^{iqn} + \\ + \frac{g}{\sqrt{N}}\sum_q\left[\sum_{l=0}^{U-1}\Gamma_l\left(2\mathrm{e}^{iqn}\phi_q + \mathrm{e}^{-i2\Omega t}\mathrm{e}^{-iqn}\phi_q^*\right)\delta_{n,n_0+l}\right], \tag{A4}$$

where $H(q) \equiv H_0 + \mathrm{e}^{iq}H_1 + \mathrm{e}^{-iq}H_1^{\dagger}$ is the Bloch matrix. This matrix has $i = 1,\ldots,\nu$ eigenvalues λ_q^i and eigenvectors v_q^i, where $\lambda_q^1 = E_{FB}$ and $v_q^i = w_q$. Let us multiply Eq. (A4) by $\frac{1}{\sqrt{N}}\mathrm{e}^{-i\hat{q}n}$ and sum over the lattice $\sum_{n=1}^{N}$. This yields to

$$i\frac{\partial}{\partial t}\sum_q \phi_q\left[\frac{1}{N}\sum_{n=1}^{N}\mathrm{e}^{i(q-\hat{q})n}\right] = \sum_q H(q)\phi_q\left[\frac{1}{N}\sum_{n=1}^{N}\mathrm{e}^{i(q-\hat{q})n}\right] + \\ + \frac{g}{N}\sum_q\left[\sum_{l=0}^{U-1}\Gamma_l\left(2\mathrm{e}^{i(q-\hat{q})(n_0+l)}\phi_q + \right.\right. \\ \left.\left. + \mathrm{e}^{-i2\Omega t}\mathrm{e}^{-i(q+\hat{q})(n_0+l)}\phi_q^*\right)\delta_{n,n_0+l}\right]. \tag{A5}$$

Without loss of generality, we choose $n_0 = 0$. The relation

$$\frac{1}{N}\sum_n e^{iqn} = \delta_{q,0} \tag{A6}$$

yields to Eq. (17) in Sec. 3.1:

$$i\dot{\phi}_{\hat{q}} = H(\hat{q})\phi_{\hat{q}} + \\ + \frac{g}{N}\sum_q \left[\sum_{l=0}^{U-1} e^{-i\hat{q}l}\Gamma_l \left(2e^{iql}\phi_q + e^{-i2\Omega t}e^{-iql}\phi_q^*\right)\right]. \tag{A7}$$

Let us now expand $\phi_{\hat{q}}$ in the Bloch eigenbasis

$$\phi_{\hat{q}} = f_{\hat{q}} w_{\hat{q}} + \sum_{i=2}^{\nu} d_{\hat{q}}^i v_{\hat{q}}^i, \tag{A8}$$

where $f_q, d_{\hat{q}}^i \in \mathbb{C}$ are time-dependent complex numbers. Equation (A7) becomes

$$i\frac{\partial}{\partial t}\left(f_{\hat{q}} w_{\hat{q}} + \sum_{i=2}^{\nu} d_{\hat{q}}^i v_{\hat{q}}^i\right) = E_{FB} f_{\hat{q}} w_{\hat{q}} + \sum_{i=2}^{\nu} \lambda_{\hat{q}}^i d_{\hat{q}}^i v_{\hat{q}}^i + \\ + \frac{g}{N}\sum_q \left\{\sum_{l=0}^{U-1} e^{-i\hat{q}l}\Gamma_l \left[2e^{iql}\left(f_q w_q + \sum_{i=2}^{\nu} d_q^i v_q^i\right) + \right.\right. \\ \left.\left. + e^{-i2\Omega t}e^{-iql}\left(f_q^* w_q + \sum_{i=2}^{\nu} d_q^{i*} v_q^i\right)\right]\right\}. \tag{A9}$$

Next, we regroup Eq. (A9) in terms of $f_{\hat{q}}$ and $d_{\hat{q}}^i$ and we multiply it by w_q^*. By the orthogonality of the eigenvectors w_q and v_q^i of the Bloch matrix $H(q)$, we obtain Eq. (19) for the flat-band component f_q

$$i\dot{f}_{\hat{q}} = E_{FB} f_{\hat{q}} + \\ + \frac{g}{N}\sum_q \left\{\sum_{l=0}^{U-1} e^{-i\hat{q}l}\left(2e^{iql} f_q + e^{-i2\Omega t}e^{-iql} f_q^*\right)\Gamma_l w_q \cdot w_q^* + \right. \\ \left. + \sum_{l=0}^{U-1}\left[\sum_{i=2}^{\nu} e^{-i\hat{q}l}\left(2e^{iql} d_q^i + e^{-i2\Omega t}e^{-iql} d_q^{i*}\right)\Gamma_l v_q^i \cdot w_q^*\right]\right\}. \tag{A10}$$

Analogously, we obtain Eq. (20) for the dispersive bands component $d_{\hat{q}}^i$ by multiplying Eq. (A9) by v_q^{j*} and using the orthogonality of the eigenvectors of the Bloch matrix $H(q)$:

$$\dot{d}_{\hat{q}}^j = \lambda_{\hat{q}}^j d_{\hat{q}}^j + \\ + \frac{g}{N}\sum_q \left\{\sum_{l=0}^{U-1} e^{-i\hat{q}l}\left(2e^{iql} f_q + e^{-i2\Omega t}e^{-iql} f_q^*\right)\Gamma_l w_q \cdot v_q^{j*} + \right. \\ \left. + \sum_{l=0}^{U-1}\left[\sum_{i=2}^{\nu} e^{-i\hat{q}l}\left(2e^{iql} d_q^i + e^{-i2\Omega t}e^{-iql} d_q^{i*}\right)\Gamma_l v_q^i \cdot v_q^{j*}\right]\right\}. \tag{A11}$$

Appendix B: Strained coefficient method

Let us consider Eq. (24) in Sec. 3.3.1 for a class $U = 1$ flat-band network

$$i\dot{f}_{\hat{q}} = E_{FB} f_{\hat{q}} + \frac{g}{N}\sum_q \left(2e^{iql} f_q + e^{-i2\Omega t}e^{-iql} f_q^*\right), \\ i\dot{d}_{\hat{q}}^j = \lambda_{\hat{q}}^j d_{\hat{q}}^j + \frac{g}{N}\sum_{i=2}^{\nu}\left\{\sum_q 2d_q^i + e^{-i2\Omega t} d_q^{i*}\right\}\Gamma_0 v_q^i \cdot v_q^{j*}, \tag{B1}$$

and the expansion of $d_{\hat{q}}$ and $\lambda_{\hat{q}}$ in Eq. (26)

$$d_{\hat{q}} = \sum_{k=0}^{+\infty} g^k u_k^{(\hat{q})}, \qquad \lambda_{\hat{q}} = m\Omega + \sum_{l=1}^{+\infty} g^l \delta_l. \tag{B2}$$

This expansion yields to

$$i\frac{\partial}{\partial t}\sum_{k=0}^{+\infty} g^k u_k^{(\hat{q})} = m\Omega\sum_{k=0}^{+\infty} g^k u_k^{(\hat{q})} + \sum_{k=0}^{+\infty}\sum_{l=1}^{+\infty} g^{k+l}\delta_l u_k^{(\hat{q})} + \\ + \frac{1}{N}\sum_{k=0}^{+\infty} g^{k+1}\left\{\sum_q \left(2u_k^{(q)} + e^{-i2\Omega t} u_k^{(q)*}\right)\right\}. \tag{B3}$$

Next, we equate the coefficients of each power of g to zero. From g^0 we get

$$iu_0^{(\hat{q})} = m\Omega u_0^{(\hat{q})} \Rightarrow u_0^{(\hat{q})}(t) = e^{-im\Omega t} a_0^{(\hat{q})}. \tag{B4}$$

Without loss of generality, we can assume all the initial conditions to be equal $a_0^{(\hat{q})} \equiv a_0$. For g^1 in Eq. (B3) we get

$$iu_1^{(\hat{q})} = m\Omega u_1^{(\hat{q})} + \delta_1 u_0^{(\hat{q})} + \frac{1}{N}\sum_q \left(2u_0^{(q)} + e^{-i2\Omega t} u_0^{(q)*}\right) \tag{B5}$$

which, by Eq. (B4), reads

$$iu_1^{(\hat{q})} = m\Omega u_1^{(\hat{q})} + \\ + \frac{1}{N}\left[(N\delta_1 + 2)e^{-im\Omega t} a_0 + e^{-i\Omega(2-m)t} a_0 + \right. \\ \left. + \sum_{q\neq\hat{q}}\left(2e^{-i\lambda_q t} a_0 + e^{-i(2\Omega-\lambda_q)t} a_0^*\right)\right]. \tag{B6}$$

Using the general solution

$$y(t) = e^{\int_0^t a(s)ds} + \int_0^t e^{\int_r^t a(s)ds} b(r)dr \tag{B7}$$

of the first-order differential equation $\dot{y}(t) = a(t)y(t) + b(t)$, for $m \neq 1$ it follows that

$$u_1^{(\hat{q})}(t) = \mathrm{e}^{-im\Omega t}a_1 + \frac{1}{N}\left(N\delta_1 + 2\right)a_0\mathrm{e}^{-im\Omega t}t + \\ + \frac{ia_0^*}{2\Omega(1-m)}\left(\mathrm{e}^{-i2\Omega t} - \mathrm{e}^{-im\Omega t}\right) + \\ + \sum_{q\neq\hat{q}}\left[\frac{i2a_0}{m\Omega-\lambda_q}\left(\mathrm{e}^{-i\lambda_q t} - \mathrm{e}^{-im\Omega t}\right) + \right. \\ \left. + \frac{ia_0^*}{\Omega(2-m)-\lambda_q}\left(\mathrm{e}^{-i(2\Omega-\lambda_q)t} - \mathrm{e}^{-im\Omega t}\right)\right]. \quad \text{(B8)}$$

To kill the secular term we need to set $\delta_1 = -2/N$ in the second term of the right-hand inside of Eq. (B8). The solution (B7) in the case $m = 1$ reads

$$u_1^{(\hat{q})}(t) = \mathrm{e}^{-i\Omega t}a_1 + \frac{1}{N}\left[\left(N\delta_1 + 2\right)a_0 + a_0^*\right]\mathrm{e}^{-i\Omega t}t + \\ + \sum_{q\neq\hat{q}}\left[\frac{i2a_0}{\Omega-\lambda_q}\left(\mathrm{e}^{-i\lambda_q t} - \mathrm{e}^{-i\Omega t}\right) + \right. \\ \left. + \frac{ia_0^*}{\Omega-\lambda_q}\left(\mathrm{e}^{-i(2\Omega-\lambda_q)t} - \mathrm{e}^{-i\Omega t}\right)\right]. \quad \text{(B9)}$$

To kill the secular term we need to set

$$(N\delta_1 + 2)a_0 + a_0^* = 0$$

$$\Leftrightarrow N\delta_1 = -2 - \frac{a_0^*}{a_0} = -2 + \mathrm{e}^{i\theta_0}$$

$$\Leftrightarrow \delta_1 = \left\{-\frac{3}{N}, -\frac{1}{N}\right\} \quad \text{(B10)}$$

since $a_0 = I_0\mathrm{e}^{i\theta_0}$, and the coefficients $\{\delta_i\}_i$ in Eq. (B2) are real numbers. The very same procedure discussed above for the components $d_{\hat{q}}$ of the dispersive states can be repeated for the component $f_{\hat{q}}$ of the flat band. Analogously to the expansion (B2), we perform an expansion for the flat-band component $f_{\hat{q}}$ in Eq. (B1):

$$f_{\hat{q}} = \sum_{k=0}^{+\infty} g^k v_k^{(\hat{q})}, \qquad E_{FB} = m\Omega + \sum_{l=1}^{+\infty} g^l \sigma_l. \quad \text{(B11)}$$

This ultimately lead to the expansion coefficients

$$\begin{aligned} &\sigma_1 = -3, -1, \quad m = 1, \\ &\sigma_1 = -2, \qquad\quad m \neq 1. \end{aligned} \quad \text{(B12)}$$

The system size N is absent due to the macroscopic degeneracy of the flat-band states. Therefore, in Eq. (B6) all terms of the sum $\sum_{q\neq\hat{q}}$ have the same time-dependent term $\mathrm{e}^{-iE_{FB}t}$. To kill the secular term in Eq. (B8) for the flat-band component f_q for $m \neq 1$, the following condition has to be satisfied

$$\sigma_1 = -\frac{1}{b_0}\frac{2}{N}\sum_q b_0 = -2. \quad \text{(B13)}$$

In Eq. (B9) for the flat-band component f_q for $m = 1$, in order to kill the secular term we need to set

$$\sigma_1 = -\frac{1}{b_0}\frac{1}{N}\left[2\sum_q b_0 + \sum_q b_0^*\right] = -2 + \mathrm{e}^{i\theta_0}$$

$$\Leftrightarrow \sigma_1 = \{-3, -1\}. \quad \text{(B14)}$$

For flat-band networks of larger class $U \geq 2$, both expansions (B2), (B11) have to be applied to Eqs. (19), (20). For the saw-tooth case, these equations reduces to Eqs. (30), (31) here recalled

$$i\dot{f}_{\hat{q}} = E_{FB}f_{\hat{q}} + \frac{g}{\alpha^2 N}\sum_q\left\{\left(\alpha^2 - 1\right)\left(f_q + \mathrm{e}^{-i2\Omega t}f_q^*\right) + \right. \\ + \mathrm{e}^{-i\hat{q}}\left(2\mathrm{e}^{iq}f_q + \mathrm{e}^{-i2\Omega t}\mathrm{e}^{-iq}f_q^*\right) + \\ \left. + \left(1 + \mathrm{e}^{-iq}\right)\left(2d_q^i + \mathrm{e}^{-i2\Omega t}d_q^{i*}\right)\right\}, \quad \text{(B15)}$$

$$i\dot{d}_{\hat{q}} = \lambda_{\hat{q}}d_{\hat{q}} + \frac{g}{\alpha^2 N}\sum_q\left\{\left(2d_q + \mathrm{e}^{-i2\Omega t}d_q^*\right) + \right. \\ + \mathrm{e}^{-i\hat{q}}\left(2\mathrm{e}^{iq}d_q + \mathrm{e}^{-i2\Omega t}\mathrm{e}^{-iq}d_q^*\right) + \\ \left. + \left(1 + \mathrm{e}^{iq}\right)\left(2f_q + \mathrm{e}^{-i2\Omega t}f_q^*\right)\right\}, \quad \text{(B16)}$$

since in the saw-tooth is a two band problem $\nu = 2$ with the following Bloch vectors w_q, v_q and projector operators Γ_0, Γ_1

$$\begin{aligned} w_q &= \frac{1}{\alpha}\begin{pmatrix} -1 \\ 1+\mathrm{e}^{iq}\end{pmatrix}, \quad \Gamma_0 = \begin{pmatrix} 0 & 0 \\ 0 & 1\end{pmatrix}, \\ v_q &= \frac{1}{\alpha}\begin{pmatrix} 1+\mathrm{e}^{-iq} \\ 1\end{pmatrix}, \quad \Gamma_1 = \begin{pmatrix} 1 & 0 \\ 0 & 1\end{pmatrix}, \end{aligned} \quad \text{(B17)}$$

where $\alpha = \sqrt{3 + 2\cos q}$. Eqs. (B15), (B16) expanded via Eqs. (B2), (B11) lead to additional time-periodic terms dependent on the wave number q (called *polarized terms*). These terms therefore do not influence the zeroing condition of the secular term presented above for class $U = 1$ flat-band networks.

Appendix C: Bogoliubov expansion

Let us consider Eq. (24) for the dispersive component d_q^i for one of the dispersive band i considered for one component only

$$i\dot{d}_q^i = \lambda_q^i d_q^i + \frac{g}{N}\left[2d_q^i + \mathrm{e}^{-i2\Omega t}d_q^{i*}\right]. \quad \text{(C1)}$$

Let us simplify the notation, by dropping the i. We now apply the Bogoliubov expansion to Eq. (C1)

$$d_q = a_q\mathrm{e}^{-i\omega t} + b_q^*\mathrm{e}^{-i(2\Omega-\omega)t}. \quad \text{(C2)}$$

This yields to

$$\omega a_q e^{-i\omega t} + (2\Omega - \omega) b_q^* e^{-i(2\Omega-\omega)t} =$$

$$= \lambda_q a_q e^{-i\omega t} + \lambda_q b_q^* e^{-i(2\Omega-\omega)t} +$$

$$+ \frac{g}{N}\left[\left(2a_q + b_q\right)e^{-i\omega t} + \left(2b_q^* + a_q^*\right)e^{-i(2\Omega-\omega)t}\right] \quad \text{(C3)}$$

which can be decoupled in two equations:

$$\omega a_q = \lambda_q a_q + \frac{g}{N}\left(2a_q + b_q\right),$$

$$\left(2\Omega - \omega\right) b_q^* = \lambda_q b_q^* + \frac{g}{N}\left(2b_q^* + a_q^*\right). \quad \text{(C4)}$$

In matrix form, Eq. (C4) reads

$$\omega \begin{pmatrix} a_q \\ b_q \end{pmatrix} = \begin{pmatrix} \tilde{\lambda} & \varepsilon \\ -\varepsilon & 2\Omega - \tilde{\lambda} \end{pmatrix} \begin{pmatrix} a_q \\ b_q \end{pmatrix} \quad \text{(C5)}$$

for $\tilde{\lambda} = \lambda_q + 2g/N$ and $\varepsilon = g/N$. The eigenvalues of this system

$$\omega_{1,2} = \Omega \pm \sqrt{\Omega^2 - 2\tilde{\lambda}\Omega + \tilde{\lambda}^2 - \varepsilon^2}. \quad \text{(C6)}$$

The argument of the square root is equal to zero when

$$\Omega_{1,2} = \frac{2\tilde{\lambda} \pm \sqrt{4\tilde{\lambda}^2 - 4(\tilde{\lambda}^2 - \varepsilon^2)}}{2} = \tilde{\lambda} \pm \varepsilon. \quad \text{(C7)}$$

This yields complex eigenvalues ω in Eq. (C3) for $\tilde{\lambda} - \varepsilon \le \Omega \le \tilde{\lambda} + \varepsilon$ which translates into

$$\lambda_q + \frac{g}{N} \le \Omega \le \lambda_q + \frac{3g}{N} \quad \text{(C8)}$$

which is the Arnold tongue obtained in Eq. (27).

Appendix D: Numerical methods

In the linear stability analysis of the compact discrete breathers, the nonlinear model (6) is reduced to the eigenvalue problem (14) of small perturbation ε_n added to a compact discrete breathers $C_{n,n_0}(t)$. We solve this problem numerically by applying an IMSL Fortran routine called DEVCRG (see [43] for details). The time evolution of the perturbed compact discrete breathers has been obtained by direct integration (for example, [38]). These numerical simulations have been performed using a 6th order Runge–Kutta procedure.

1. D. Leykam, A. Andreanov, and S. Flach, *Adv. Phys. X* in print (2018), *arXiv preprint arXiv:1801.09378* (2018).
2. B. Sutherland, *Phys. Rev. B* **34**, 5208 (1986).
3. E.H. Lieb, *Phys. Rev. Lett.* **62**, 1201 (1989).
4. A. Mielke, *J. Phys. A: Math. Gen.* **24**, 3311 (1991).
5. H. Tasaki, *Phys. Rev. Lett.* **69**, 1608 (1992).
6. E.J. Bergholtz and Z. Liu, *Int. J. Mod. Phys. B* **27**, 1330017 (2013).
7. O. Derzhko, J. Richter, and M. Maksymenko, *Int. J. Mod. Phys. B* **29**, 1530007 (2015).
8. R. Moessner and A.P. Ramirez, *Phys. Today* **59**, 24 (2006).
9. J.D. Bodyfelt, D. Leykam, C. Danieli, X. Yu, and S. Flach, *Phys. Rev. Lett.* **113**, 236403 (2014).
10. C. Danieli, J.D. Bodyfelt, and S. Flach, *Phys. Rev. B* **91**, 235134 (2015).
11. D. Leykam, S. Flach, O. Bahat-Treidel, and A.S. Desyatnikov, *Phys. Rev. B* **88**, 224203 (2013).
12. D. Leykam, S. Flach, and Y.D. Chong, *Phys. Rev. B* **96**, 064305 (2017).
13. A.R. Kolovsky, A. Ramachandran, and S. Flach, *Phys. Rev. B* **97**, 045120 (2018).
14. R. Khomeriki and S. Flach, *Phys. Rev. Lett.* **116**, 245301 (2016).
15. A. Ramachandran, C. Danieli, and S. Flach, *arXiv preprint arXiv:1801.03210* (2018).
16. S. Flach and R. Khomeriki, *Sci. Rep.* **7**, 40860 (2017).
17. S. Peotta and P. Törmä, *Nat. Commun.* **6**, 8944 (2015).
18. A. Ramachandran, A. Andreanov, and S. Flach, *Phys. Rev. B* **96**, 161104 (2017).
19. R.G. Dias and J.D. Gouveia, *Sci. Rep.* **5**, 16852 (2015).
20. L. Morales-Inostroza and R.A. Vicencio, *Phys. Rev. A* **94**, 043831 (2016).
21. S. Flach, D. Leykam, J.D. Bodyfelt, P. Matthies, and A.S. Desyatnikov, *Europhys. Lett.* **105**, 30001 (2014).
22. W. Maimaiti, A. Andreanov, H.C. Park, O. Gendelman, and S. Flach, *Phys. Rev. B* **95**, 115135 (2017).
23. S. Taie, H. Ozawa, T. Ichinose, T. Nishio, S. Nakajima, and Y. Takahashi, *Sci. Adv.* **1**, e1500845 (2015).
24. R.A. Vicencio, C. Cantillano, L. Morales-Inostroza, B. Real, C. Mejía-Cortés, S. Weimann, A. Szameit, and M.I. Molina, *Phys. Rev. Lett.* **114**, 245503 (2015).
25. S. Mukherjee, A. Spracklen, D. Choudhury, N. Goldman, P. Öhberg, E. Andersson, and R.R. Thomson, *Phys. Rev. Lett.* **114**, 245504 (2015).
26. S. Weimann, L. Morales-Inostroza, B. Real, C. Cantillano, A. Szameit, and R.A. Vicencio, *Opt. Lett.* **41**, 2414 (2016).
27. N. Masumoto, N.Y. Kim, T. Byrnes, K. Kusudo, A. Löffler, S. Höfling, A. Forchel, and Y. Yamamoto, *New J. Phys.* **14**, 065002 (2012).
28. F. Baboux, L. Ge, T. Jacqmin, M. Biondi, E. Galopin, A. Lemaître, L. Le Gratiet, I. Sagnes, S. Schmidt, H.E. Türeci, A. Amo, and J. Bloch, *Phys. Rev. Lett.* **116**, 066402 (2016).
29. J. Vidal, R. Mosseri, and B. Douçot, *Phys. Rev. Lett.* **81**, 5888 (1998).
30. C. Abilio, P. Butaud, T. Fournier, B. Pannetier, J. Vidal, S. Tedesco, and B. Dalzotto, *Phys. Rev. Lett.* **83**, 5102 (1999).
31. S. Flach and C.R. Willis, *Phys. Rep.* **295**, 181 (1998).
32. S. Flach and A.V. Gorbach, *Phys. Rep.* **467**, 1 (2008).
33. P. Rosenau and J.M. Hyman, *Phys. Rev. Lett.* **70**, 564 (1993).
34. J. Page, *Phys. Rev. B* **41**, 7835 (1990).
35. P. Kevrekidis and V. Konotop, *Phys. Rev. E* **65**, 066614 (2002).
36. M. Johansson, U. Naether, and R.A. Vicencio, *Phys. Rev. E* **92**, 032912 (2015).

37. P. Beličev, G. Gligorić, A. Maluckov, M. Stepić, and M. Johansson, *Phys. Rev. A* **96**, 063838 (2017).
38. G. Gligorić, A. Maluckov, L. Hadžievski, S. Flach, and B.A. Malomed, *Phys. Rev. B* **94**, 144302 (2016).
39. N. Perchikov and O. Gendelman, *Phys. Rev. E* **96**, 052208 (2017).
40. A. Nayfeh, *Introduction to Perturbation Theory*, New York: Wiley (1993).
41. J. Marín and S. Aubry, *Physica D: Nonlinear Phenomena* **119**, 163 (1998).
42. A.J. Lichtenberg and M.A. Lieberman, *Regular and Chaotic Dynamics*, Vol. 38 of App. Math. Sci.; Springer-Verlag: Berlin (1992).
43. V. Numerics, Imsl Fortran Library User Guide Mathematical Functions in Fortran, Visual Numerics, Inc. USA (2003).